# A Predictive Power Control for Wind Energy

Alfeu J. Sguarezi Filho, Milton E. de Oliveira Filho, and Ernesto Ruppert Filho

***Abstract*—The doubly fed induction generator (DFIG) is widely used in wind energy. This paper proposes a model-based predictive controller for a power control of DFIG. The control law is derived by optimization of an objective function that considers the control effort and the difference between the predicted outputs (active and reactive power) and the references. The prediction was calculated using a linearized state-space model of DFIG. As the generator leakage inductance and resistance information were required for this control method, the influence of the estimation errors for these parameters was also investigated. Simulation results are presented to validate the proposed controller.**

***Index Terms*—Doubly fed induction generator (DFIG), model-based predictive control (MBPC), power control, wind energy.**

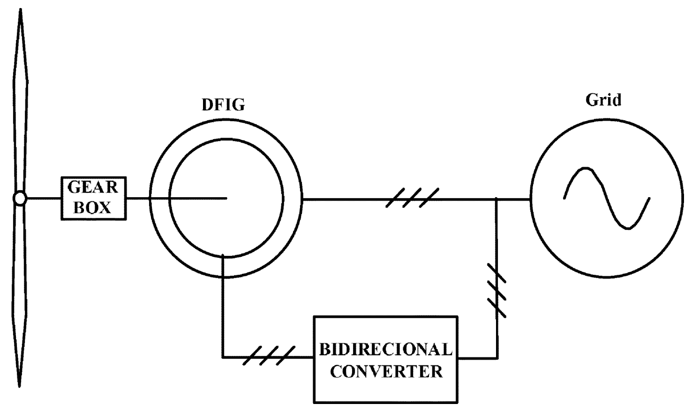


Fig. 1. Configuration of the DFIG connected directly to the grid.

## I. Introduction

RENEWABLE energy systems and especially wind energy have attracted interest as a result of the increasing concern about $CO_2$ emissions. Wind energy systems using a doubly fed induction generator (DFIG) have some advantages due to variable speed operation and four quadrant active and reactive power capabilities compared with fixed speed squirrel cage induction generators [1], [2].

The stator of DFIG is directly connected to the grid and the rotor is connected to the grid by a bidirectional converter, as shown in Fig. 1. The converter connected to the rotor controls active and the reactive power between the stator of the DFIG and ac supply or a standalone grid [3].

The control wind turbine system is traditionally based on either stator-flux-oriented [4] or stator-voltage-oriented [5], [6] vector control. The scheme decouples the rotor current into active and reactive power components. The control of the active and reactive power are achieved with a rotor current controller. Some investigations using PI controllers and stator-flux-oriented vector control have been presented by [7] and [8]. The problem in the use of PI controller is the tuning of the gains and the cross-coupling on DFIG terms in the whole operating range. Interesting methods to solve these problems have been presented by [9]–[11].

Some investigations using a predictive functional controller [12] and internal mode controller [13], [14] have satisfactory performance when compared with the response of PI, but it is difficult to implement one due to the formulation of a predictive functional controller and the internal mode controller. Another possibility to DFIG power control can be realized by using fuzzy logic [15]. These strategies have satisfactory power response, although the errors in parameters estimation can degrade the system response.

Direct power control (DPC) was based on the principles of direct torque control [16], [17]. The DPC applied to the DFIG power control has been presented in [18]–[20]. This strategy calculates the rotor voltage space vector based on stator flux estimated and power erros. In [18], the principles and the implementation of DPC are obtained with hysteresis controllers and variable switching frequency. In [19] and [20], the principles of this method are described in detail and simulations results have been presented using variable and constant switching frequency, respectively. Moreover, the conventional DPC complicates the AC filter design because of its variable switching frequency. An alternative to DPC is power error vector control [21]. This strategy is less complex and obtains results similar to those of direct control of power.

A anti-jamming control has been proposed by [22] to improve the controller performance. This control has a satisfactory performance, however, power and rotor currents results were shown only in fixed speed operation and the power control using a rotor currents loop has current overshoot as a disadvantage.

The predictive control is an alternative control technique that was applied in machine drives and inverters [23], [24]. Some investigations like long-range predictive control [25], general predictive control [23], and model predictive control [26]–[28] were applied to the induction motor drives. The predictive functional control was applied to the DFIG power control by using a rotor current loop in [12] and a predictive DPC for DFIG was presented in [29]. These strategies have a satisfactory power response although the control does not predict the outputs (active and reactive power) and the power response can be degraded.

This paper proposes a model-based predictive controller for power control of DFIG. The control law is derived by optimization of an objective function that considers the control effort and the difference between the predicted outputs (active and

Manuscript received May 04, 2010; revised September 27, 2010; accepted October 12, 2010. Date of publication October 18, 2010; date of current version December 15, 2010. This work was supported by the CAPES and FAPESP.

The authors are with University of Campinas, FEEC–DSCE, CP 6101, Campinas, Brazil (e-mail: sguarezi@dsce.fee.unicamp.br; mfilho@dsce.fee.unicamp.br; rupert@fee.unicamp.br).

Digital Object Identifier 10.1109/TSTE.2010.2088408

reactive power) and the references. The prediction was calculated using a linearized state-space model of DFIG. As the generator leakage inductance and resistance information were required for this control method, the influence of the estimation errors for these parameters was also investigated. The contribution is in applying this control technique for controlling powers of DFIG. Simulation results are presented to validate the proposed controller.

## II. Machine Model and Rotor Current Vector Control

The DFIG model in the synchronous $dq$ reference frame is given by [30]

$$\vec{v}_{1dq} = R_1\vec{i}_{1dq} + \frac{d\vec{\lambda}_{1dq}}{dt} + j\omega_1\vec{\lambda}_{1dq} \tag{1}$$

$$\vec{v}_{2dq} = R_2\vec{i}_{2dq} + \frac{d\vec{\lambda}_{2dq}}{dt} + j\left(\omega_1 - \mathrm{NP}\omega_{\mathrm{mec}}\right)\vec{\lambda}_{2dq} \tag{2}$$

where the relationship between fluxes and currents is

$$\vec{\lambda}_{1dq} = L_1\vec{i}_{1dq} + L_M\vec{i}_{2dq} \tag{3}$$

$$\vec{\lambda}_{2dq} = L_M\vec{i}_{1dq} + L_2\vec{i}_{2dq} \tag{4}$$

and generator active and reactive power are

$$P = \frac{3}{2}\left(v_{1d}i_{1d} + v_{1q}i_{1q}\right) \tag{5}$$

$$Q = \frac{3}{2}\left(v_{1q}i_{1d} - v_{1d}i_{1q}\right). \tag{6}$$

The subscripts 1 and 2 represent the stator and rotor parameters respectively, $\omega_1$ represents the synchronous speed, $\omega_{\mathrm{mec}}$ represents machine speed, $R_1$ and $R_2$ represent stator and the rotor windings per phase electrical resistance, $L_1$ , $L_2$, and $L_m$ represent the proper and the mutual inductances of the stator and rotor windings, $\vec{v}$ represents voltage vector, and NP represents the machine number of pair of poles.

The DFIG power control aims independent stator active $P$ and reactive $Q$ power control by means a rotor current regulation. For this purpose, $P$ and $Q$ are represented as functions of each individual rotor current. We use stator flux oriented control, that decouples the $dq$ axis, which means: $\lambda_{1d} = \lambda_1 = |\vec{\lambda}_{1dq}|$. Thus, (3) becomes

$$i_{1d} = \frac{\lambda_1}{L_1} - \frac{L_M}{L_1}i_{2d} \tag{7}$$

$$i_{1q} = -\frac{L_M}{L_1}i_{2q}. \tag{8}$$

Similarly, using stator flux oriented the stator voltage becomes $v_{1d} = 0$ and $v_{1q} = v_1 = |\vec{v}_{1dq}|$. Hence, the active (5) and reactive (6) power can be calculated by using (7) and (8)

$$P = -\frac{3}{2}v_1\frac{L_M}{L_1}i_{2q} \tag{9}$$

$$Q = \frac{3}{2}v_1\left(\frac{\lambda_1}{L_1} - \frac{L_M}{L_1}i_{2d}\right). \tag{10}$$

Thus, rotor currents will reflect on stator current and on stator active and reactive power, respectively. Consequently, this principle can be used on stator active and reactive power control of the DFIG.

### A. Rotor Side Equations

The rotor currents control, using (9) and (10), allows the DFIG power control. The rotor voltage (2), in the synchronous referential frame using the stator flux position, and by using (7) and (8), becomes

$$\vec{v}_{2dq} = \left(R_2 + j\sigma L_2\omega_{sl}\right)\vec{i}_{2dq} + \sigma L_2\frac{d\vec{i}_{2dq}}{dt} + j\frac{L_m}{L_1}\omega_{sl}\lambda_1 \tag{11}$$

where $\omega_{sl} = \omega_1 - \mathrm{NP}\omega_{\mathrm{mec}}$ and $\sigma = 1 - L_M^2/L_1L_2$.

In space state form, (11) becomes

$$\dot{\bar{x}} = A\bar{x} + B\bar{u} + G\bar{\omega} \tag{12}$$
$$\bar{y} = C\bar{x}$$

$$\begin{bmatrix}\frac{di_{2d}}{dt}\\ \frac{di_{2q}}{dt}\end{bmatrix} = \begin{bmatrix}\frac{-R_2}{\sigma L_2} & \omega_{sl}\\ -\omega_{sl} & \frac{-R_2}{\sigma L_2}\end{bmatrix}\begin{bmatrix}i_{2d}\\ i_{2q}\end{bmatrix} + \begin{bmatrix}\frac{1}{\sigma L_2} & 0\\ 0 & \frac{1}{\sigma L_2}\end{bmatrix}\begin{bmatrix}v_{2d}\\ v_{2q}\end{bmatrix} + \begin{bmatrix}1 & 0\\ 0 & 1\end{bmatrix}\begin{bmatrix}0\\ \frac{-\omega_{sl}L_M}{\sigma L_1L_2}\lambda_1\end{bmatrix} \tag{13}$$

where $C = I$ and $I$ the identity matrix. Thus, $C$ also represents the identity matrix.

From now on, it will be assumed that the mechanical time constant is much greater than the electrical time constants. Thus, $\omega_{\mathrm{mec}} = \text{constant}$ is a valid approximation for a sample time [31]–[33]. Since the synchronous speed $\omega_1$ is fixed by the grid and $\omega_{sl} = \omega_1 - \mathrm{NP}\omega_{\mathrm{mec}}$, the $\omega_{sl} = \text{constant}$ is also a valid approximation for a sample time.

Equation (13) can be discretized considering $T$ as the sampling period and $k$ as the sampling time by using zero-order-hold (ZOH) [32], [34] with no delay as

$$\bar{x}\left(k+1\right) = A_d\bar{x}(k) + B_d\bar{u}(k) + G_d\bar{\omega}_d(k)$$
$$\bar{y}\left(k+1\right) = C_d\bar{x}\left(k+1\right) \tag{14}$$

where

$$A_d = e^{AT} \cong I + AT$$
$$B_d = \int_0^{\tau} e^{AT}B\,d\tau \cong BT$$
$$G_d = \int_0^{\tau} e^{AT}G\,d\tau \cong GT$$
$$C_d = C. \tag{15}$$

Equation (13) can be discretized due to the rotor applied voltage is constant during a control period of the PWM voltage source inverter. Thus, the (13) discretized using (14) is given by

$$\begin{bmatrix}i_{2d}(k+1)\\ i_{2q}(k+1)\end{bmatrix} = \begin{bmatrix}1 - \frac{R_2T}{\sigma L_2} & \omega_{sl}T\\ -\omega_{sl}T & 1 - \frac{R_2T}{\sigma L_2}\end{bmatrix}\begin{bmatrix}i_{2d}(k)\\ i_{2q}(k)\end{bmatrix} + + \begin{bmatrix}\frac{T}{\sigma L_2} & 0\\ 0 & \frac{T}{\sigma L_2}\end{bmatrix}\begin{bmatrix}v_{2d}(k)\\ v_{2q}(k)\end{bmatrix} + + \begin{bmatrix}1 & 0\\ 0 & 1\end{bmatrix}\begin{bmatrix}0\\ \frac{-\omega_{sl}L_MT}{\sigma L_1L_2}\lambda_1(k)\end{bmatrix}. \tag{16}$$

## III. Model-Based Predictive Control Applied to the DFIG Power Control

The model-based predictive control (MBPC) involves a class of control techniques that consists of two main elements: the model of the system being controlled and the optimizer that determines the optimal future control actions. The system model is used to predict the future behavior of the system with control law obtained by optimizing a cost function. The cost function considers the effort needed to control the deviation between the expected and the real values.

The receding horizon principle is used for the first element of the optimal sequence is applied. In any plant, new measurements are made for each sample of success and then the procedures are repeated.

The main steps of MBPC are estimates of output and determining the control law.

There are various MBPC techniques for output prediction using the state space model or the transfer function of the system [28], [35]. In this paper, the output prediction is derived from the state space model and it is given by

$$Y = P_{px}x_k + HU + D\omega_{d_k} \tag{17}$$

where

$$Y = \left[y(k+1) \quad y(k+2) \quad \cdots \quad y(k+n_y)\right]^T \tag{18}$$

$$U = \left[u(k) \quad u(k+1) \quad \cdots \quad u(k+n_y-1)\right]^T \tag{19}$$

$$P_{px} = \left[C_dA_d \quad C_dA_d^2 \quad C_dA_d^3 \quad \cdots \quad C_dA_d^{n_y}\right]^T \tag{20}$$

$$H = \begin{bmatrix} C_dB_d & 0 & 0 & \cdots \\ C_dA_dB_d & C_dB_d & 0 & \cdots \\ C_dA_d^2B_d & C_dA_dB_d & C_dB_d & \cdots \\ \vdots & \vdots & \vdots & \vdots \\ C_dA_d^{n_y-1}B_d & C_dA_d^{n_y-2}B_d & C_dA_d^{n_y-3}B_d & \cdots \end{bmatrix} \tag{21}$$

$$D = \begin{bmatrix} C_d & 0 & 0 & \cdots & 0 \\ C_dA_d & C_d & 0 & \cdots & 0 \\ C_dA_d^2 & CA_d & C_d & \cdots & 0 \\ \vdots & \vdots & \vdots & \vdots & \\ C_dA_d^{n_y-1} & CA_d^{n_y-2} & CA_d^{n_y-3} & \cdots & C \end{bmatrix} \tag{22}$$

where $n_y$ represents the prediction horizon output, $Y$ is the predicted outputs, $x_k = \bar{x}(k)$, and $\omega_{d_k} = \bar{\omega_d}(k)$. The choice of the prediction horizon $n_y$ is critical for the performance of the control, because the selection of a high value improves the stability of the system, but may increase the computational costs excessively. Another factor that must be taken into consideration when choosing $n_y$ is the confidence implanted by the designer in the model representation of the plant. When there is no guarantee that the model precision describes the plant, smaller $n_y$ must be chosen [35].

The state variables are estimated with the rotor speed, the stator voltages, and currents measured by sensors.

The control law is obtained by minimizing the quadratic cost function which exists in the error between the prediction based on the model and future references. The quadratic function in its matrix form is given by [28]

$$J = (Y-w)^T W_y (Y-w) + U^T W_u U \tag{23}$$

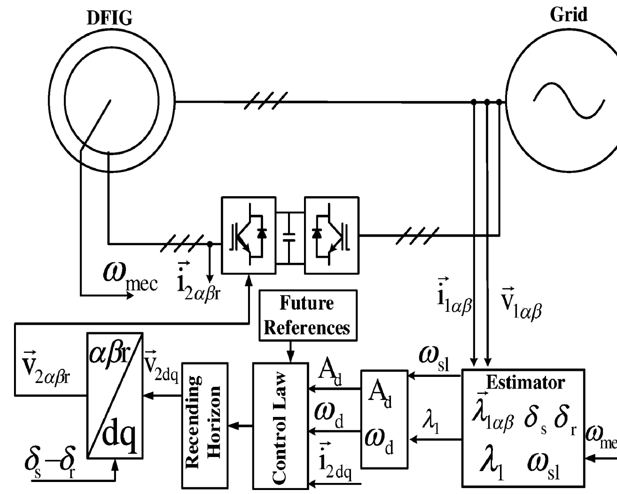


Fig. 2. Block diagram of proposed predictive power control strategy.

where $w \in R^{(n_y \times q)\times 1}$ represents the vector of the future output references to be controlled, $W_y \in R^{(n_y\times q)\times(n_y \times q)}$ stands for a positive-defined matrix that allows an emphasis on each of the controlled outputs and its predictions, $W_u \in R^{n_u \times n_u}$ stands for a positive-defined matrix, usually diagonal, which weighs the control efforts of inputs, $U \in R^{n_u \times n_u}$ is the input, $q$ is the number of outputs, and $n_u$ is the control horizon.

In the case of $n_u = 1$, the magnitude of entries represents an average value that allows the outputs to follow the references. In the case of $n_u > 1$, the control strategy generates control signals that make the output follow the reference more closely. Choosing big numbers of $n_u$ high control signals are generated and the computational costs increase excessively.

The matrix $W_u$ reflects on the control effort. The elements of $W_u$ are different from zero due to the fact that these values influence the response of the controller with high overshoot when they are void. Thus, if elements of $W_u$ are equal to zero, it means that the actuator can provide infinite energy and it does not match the actual devices that have limitations. The $W_y$ permits the emphasis of each individual prediction of the outputs that would improve the response time of the plant [35]. A method for calculating the elements of this matrix from a nonlinear system is presented in [36]. However, the computational cost involved in this procedure is significant.

In the cost function (23), the model is linearized. The minimal value of the cost function can be determined algebraically from $\partial J/\partial U = 0$. Since $P_{px}$, $H$, and $D$ depend on estimated states, they must be updated for each control cycle. The substitution of $Y$, from (17) into (23), results in a quadratic cost function, dependent on $U$, which gives the analytical optimal solution. The control law using the minimal value of the cost function is achieved making $\partial J/\partial U = 0$ and isolating $U$. Thus, this expression is given by

$$U = \left(H^TW_yH + W_u\right)^{-1} H^TW_y\left(w - P_{px}x_k - D\omega_{d_k}\right). \tag{24}$$

The diagram of the MBPC applied to the DFIG power control is shown in Fig. 2. The converter, which is connected to the grid controls the voltage of the link DC. This type of control can be accomplished by any technique for inverter control rectifier as presented in [37], [38]. The converter is designed to send or receive energy from the grid according to the operating speed of the generator. In the super-synchronous speed operation ($\omega_{\mathrm{mec}} > \omega_1$) the converter send energy to the grid and in the subsynchronous speed operation ($\omega_{\mathrm{mec}} < \omega_1$) the converter receive energy from the grid.

For the active power control, the rotor current reference using (9) is given by

$$i_{2q_{\mathrm{ref}}} = -\frac{2P_{\mathrm{ref}}L_1}{3v_1 L_M}. \tag{25}$$

The reactive power control by using (10) the rotor current reference is

$$i_{2d_{\mathrm{ref}}} = -\frac{2Q_{\mathrm{ref}}L_1}{3v_1 L_M} + \frac{\lambda_1}{L_M}. \tag{26}$$

Using (24), the MBPC algorithm, the rotor voltages that allow the active and reactive power convergence to their respective reference values are generated. The desired rotor voltage in the rotor $\alpha\beta r$ reference frame generates switching signals for the rotor side using either space vector modulation that is given by $\vec{v}_{2\alpha\beta r} = \vec{v}_{2dq}\; e^{\delta_s - \delta_r}$

Stator currents and voltages, rotor speed and currents are measured to stator flux position $\delta_s$ and magnitude $\lambda_1$, synchronous frequency $\omega_1$ and slip frequency $\omega_{sl}$ estimation.

### A. Estimation

For the predictive control, it is necessary to calculate the active and reactive power, the stator flux magnitude and position, and the slip speed and synchronous frequency. The flux estimation using (1) is given by

$$\vec{\lambda}_{1\alpha\beta} = \int \left(\vec{v}_{1\alpha\beta} - R_1\vec{i}_{1\alpha\beta}\right) dt \tag{27}$$

and the flux position by using (27) as

$$\delta_s = \arctan\left(\frac{\lambda_{1\beta}}{\lambda_{1\alpha}}\right). \tag{28}$$

The synchronous speed $\omega_1$ estimation is given by

$$\omega_1 = \frac{d\delta_s}{dt} = \frac{(v_{1\beta} - R_1 i_{1\beta})\,\lambda_{1\alpha} - (v_{1\alpha} - R_1 i_{1\alpha})\,\lambda_{1\beta}}{(\lambda_{1\alpha})^2 + (\lambda_{1\beta})^2} \tag{29}$$

and the slip speed estimation by using the rotor speed and synchronous speed is

$$\omega_{sl} = \omega_1 - \mathrm{NP}\omega_{\mathrm{mec}}. \tag{30}$$

The angle in rotor reference frame is given by

$$\delta_s - \delta_r = \int \omega_{sl} dt. \tag{31}$$

## IV. Impact of Parameter Variations on System Performance

The analysis of the impact of parameter variations was made by using (16), (24), (25), and (26), which allows rotor voltage calculation. The stator resistance used in stator flux estimation and the rotor resistance used in rotor voltage calculation have negligible impact on the system performance for high-power generators [5], [20]. The accuracy of the rotor voltage calculation is influenced by the constant $\sigma L_2$ and the inductance ratio $L_1/L_M$ that are determined by the stator and rotor leakage and magnetization inductance. Since the leakage flux magnetic path is mainly air, the variation of the leakage inductance during operation is insignificant. However, magnetization inductance variation needs to be considered due to possible variation of the magnetic permeability of the stator and rotor cores under different operating conditions. The required parameters can be simplified considering the relatively small leakage inductance $L_{l1}$ and $L_{l2}$ compared to the magnetization inductance $L_m$ which is shown in Appendix and given by

$$\sigma L_2 \cong (L_{l1} + L_{l2}),\; \frac{L_1}{L_M} = \frac{L_M + L_{l1}}{L_M} \cong 1. \tag{32}$$

Equation (32) shows that the variations of $L_M$ has little impact in $\sigma L_2$ and $L_1/L_M$, and therefore, its influence on the performance of the proposed control strategy would also be insignificant.

## V. Simulation Results

The simulation of proposed control strategy used the MATLAB/SimPowerSystems package. The power control strategy has a $T = 0.3\; 10^{-4}s$ and the sampling time of the voltage source inverter is $T = 0.5\; 10^{-4}s$. The DFIG parameters are shown in the Appendix. Fig. 2 shows the scheme of the implemented system. To the power factor (PF) control, the reactive power reference is given by

$$Q_{\mathrm{ref}} = P_{\mathrm{ref}}\frac{\sqrt{1-\mathrm{PF}^2}}{\mathrm{PF}}.$$

In the predictive controller, if $n_y$ is increased, the output dynamic is slower. The elements of the matrices $W_u$ and $W_y$ weights should be adjusted carefully so that they meet the requirements desired by the designer. It is known that the matrix $W_u$ is related to the control effort and its elements must be nonzero because it causes high overshoot. Already matrix $W_y$ emphasizes each individual prediction of the output that would improve the response time of the plant. From studies conducted by simulation with $n_u = 1$, settling time less than 10 ms and overshoot less than 10%, the matrices $W_u$ and $W_y$ are given by

$$W_y = \begin{bmatrix} 15 & 0 \\ 0 & 45 \end{bmatrix} \quad \text{and} \quad W_u = \begin{bmatrix} 0.002 & 0 \\ 0 & 0.01 \end{bmatrix}.$$

Initial studies with various active and reactive power steps and constant rotor speed at 226.6 rad/s were carried out to testthe dynamic response of the proposed power control strategy, shown in Fig. 3(a). A detailed power response shown in Fig. 4, demonstrates an overshoot less than 10% and a settling time less than 5 ms. The initial active power and the power factor references were $-60$ kW and PF $= +0.85$. The active power and the power factor references were step changed from $-60$ to $-100$ kW and from PF of 0.85 to $-0.85$ at 1.75 s. The power reference was step changed again from $-100$ to $-149.2$ kW and from PF of $-0.85$

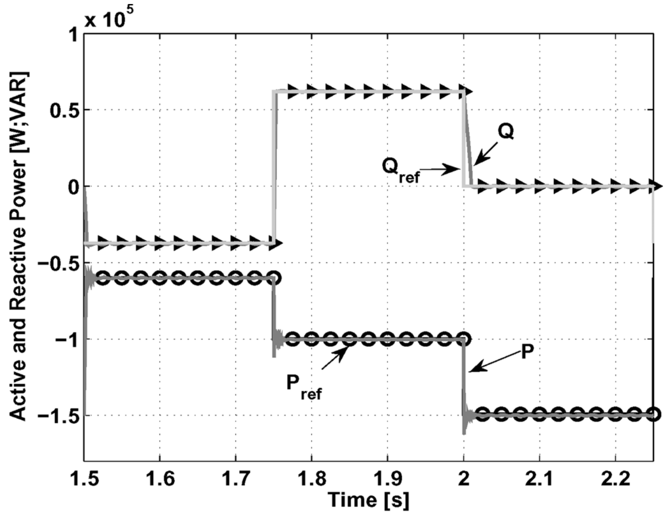

(a)

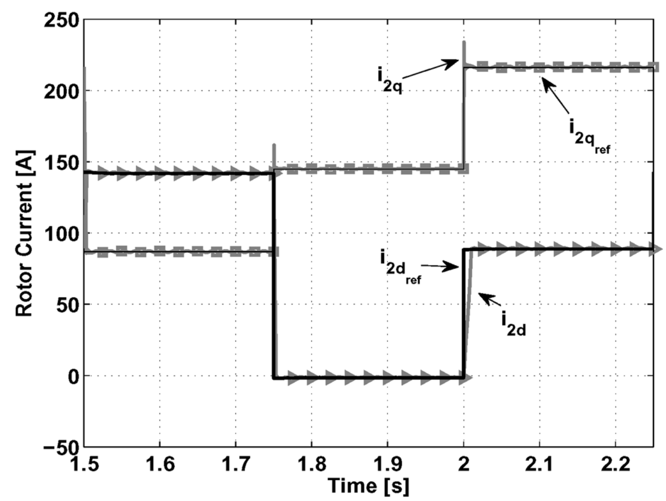

(b)

Fig. 3. Response of step tests for active and reactive power and rotor currents in supersynchronous operation. (a) Response of step of active and reactive power. (b) Response of step of rotor currents in synchronous referential.

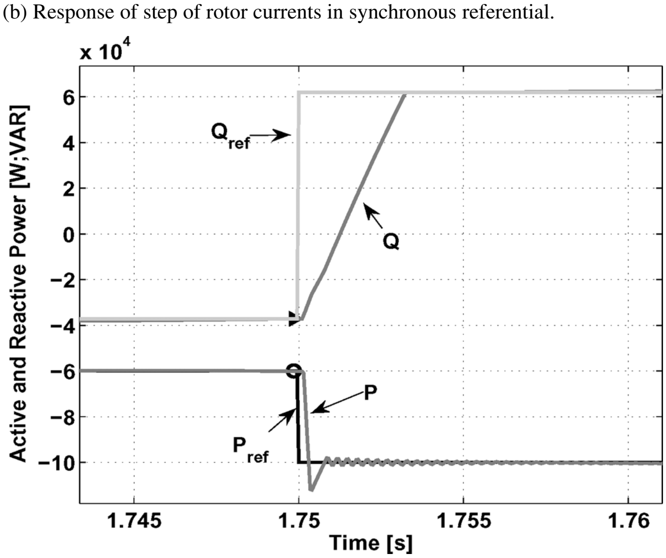


Fig. 4. Detailed power response.

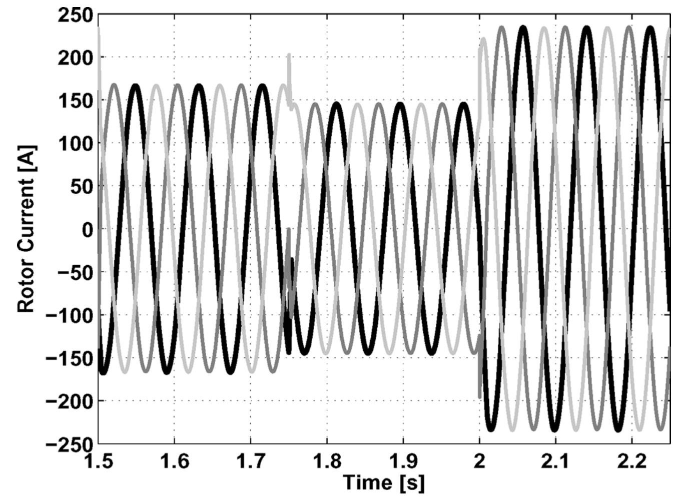

(a)

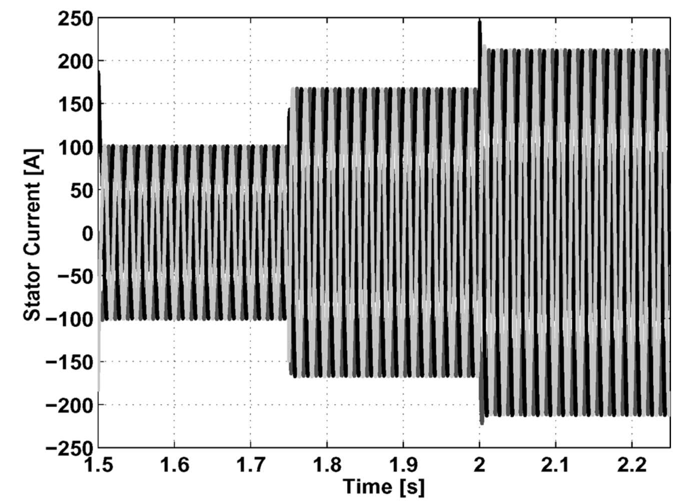

(b)

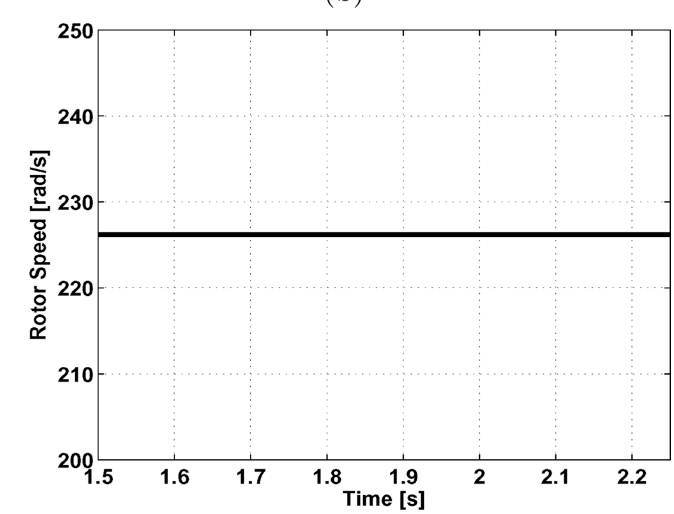

(c)

Fig. 5. (a) Rotor currents. (b) Stator currents. (c) Rotor speed.

to 1 at 2 s, respectively. The rotor currents in synchronous reference is shown in Fig. 3(b) and the rotor speed, the rotor and stator currents in the stationary reference are shown in Fig. 5. The dynamic response of both active and reactive power is less than 10 ms; there is overshoot less than 10% of either stator/rotor or the active/reactive powers. The satisfactory performance of

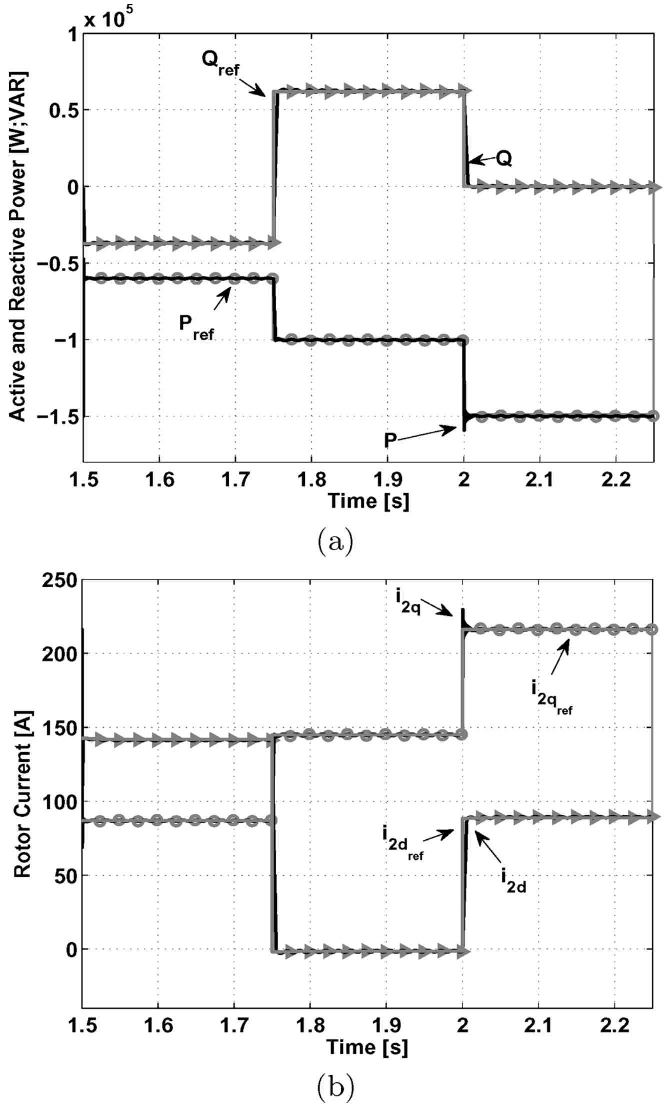


Fig. 6. Response of step tests for active and reactive power and rotor currents with several speed operation. (a) Response of step of active and reactive power. (b) Response of step of rotor currents in synchronous referential.

the controller can be seen due to the fact that the controller performance is in accordance with the design parameters.

Several studies using different power steps and rotor speed were carried out to test the proposed power control strategy. During the period 1.75–2.1 s, the rotor speed increased from 151.1 to 226.6 rad/s. Fig. 6(a) shows the results of the step reference tests of active and reactive power. The power steps, i.e., the active power and the power factor references were changed from $-60$ to $-100$ kW and the PF of 0.85 to $-0.85$ at 1.75 s. The rotor currents in synchronous reference are shown in Fig. 6(b) and the rotor speed, the rotor and stator currents at the stationary reference are shown in Fig. 7, and the voltage of the capacitor is presented in Fig. 8. The satisfactory performance of the controller can be verified considering that the active and the reactive power reach the desired reference values when the rotor speed varies.

The rotor resistance $R_2$ and the mutual inductance $L_M$ are increased by 20% in order to test the impact of the parameter

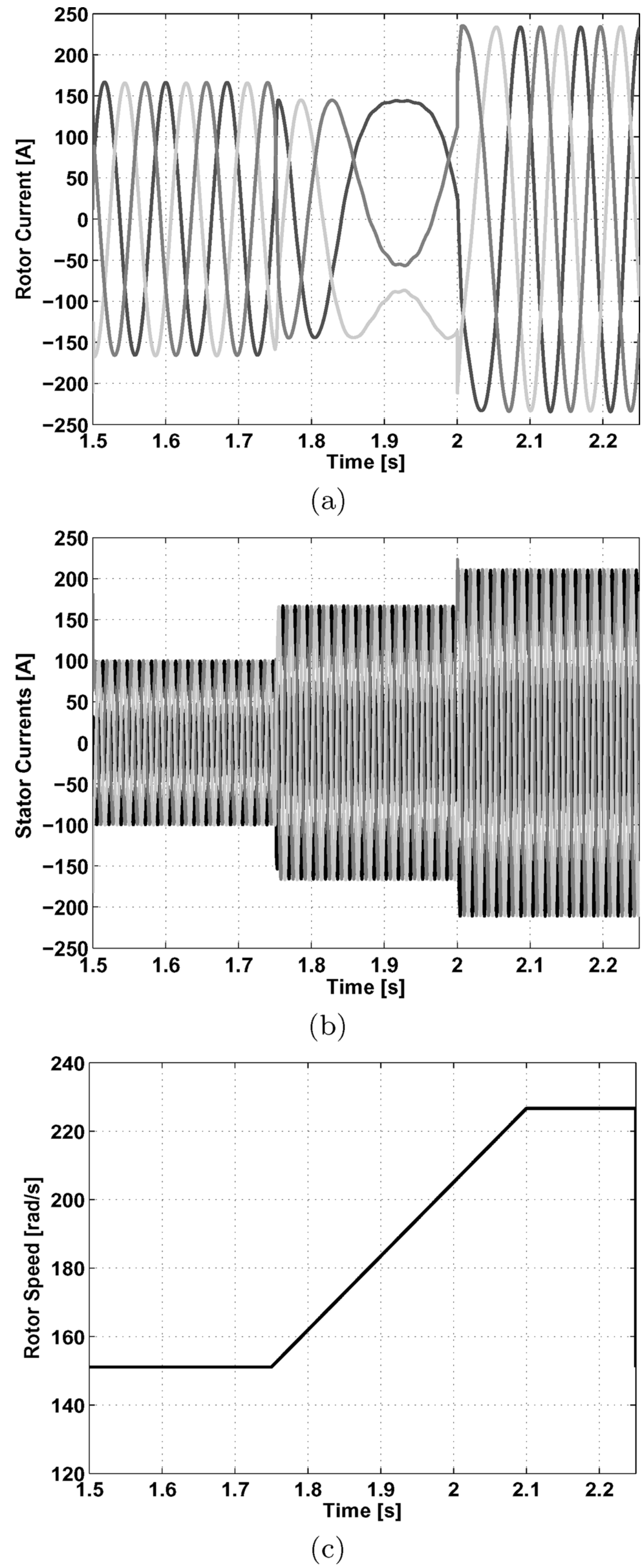


Fig. 7. Stator and rotor currents and rotor speed with several speed operation. (a) Rotor currents. (b) Stator currents. (c) Rotor speed.

variations on the system performance. The same tests of step reference of active and reactive powers with rotor speed variation and with parameter variation are shown in Figs. 9 and 10.

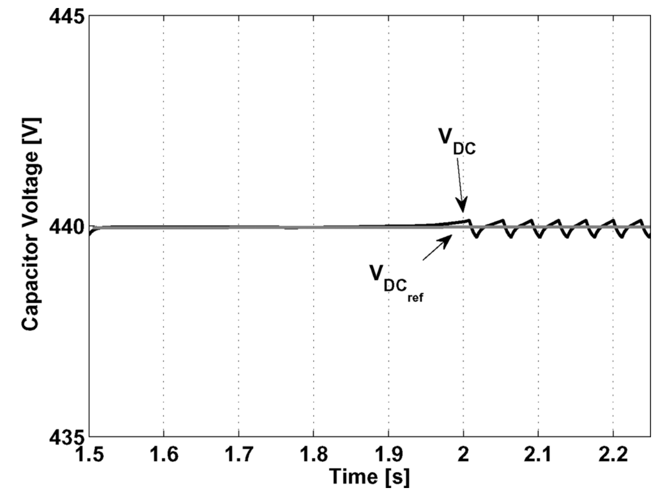


Fig. 8. DC link voltage.

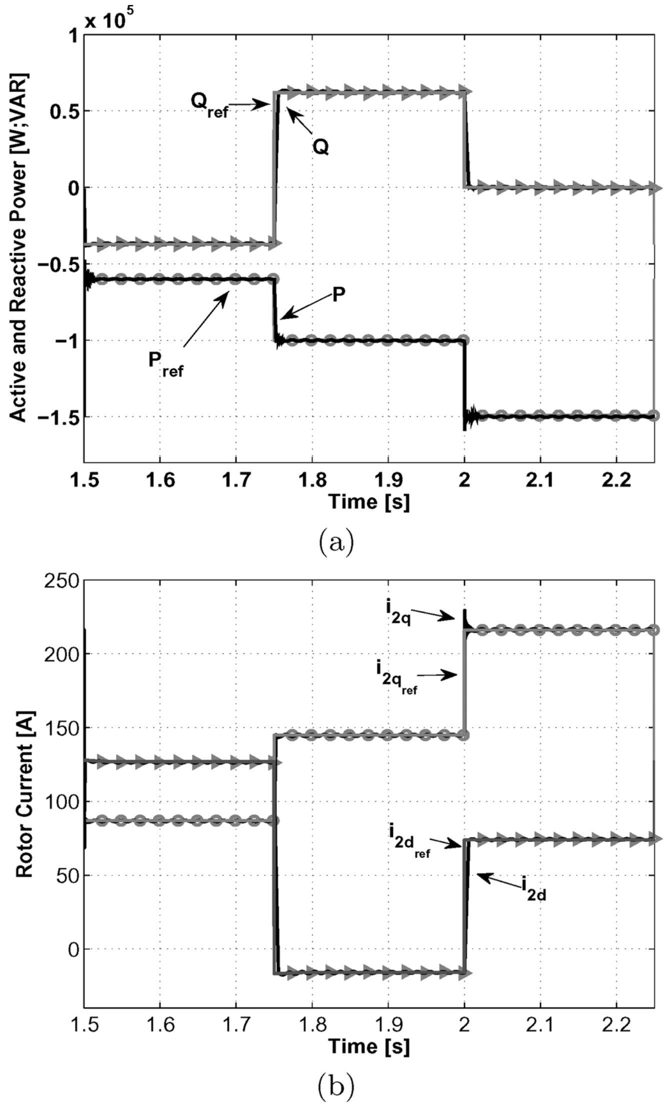


Fig. 9. Response of step tests for active and reactive power and rotor currents with several speed operation and parameters variations. (a) Response of step of active and reactive power. (b) Response of step of rotor currents in synchronous referential.

Comparing Figs. 6 and 9 and Figs. 7 and 10, there can hardly be noticed any difference, and even with large inductance and rotor

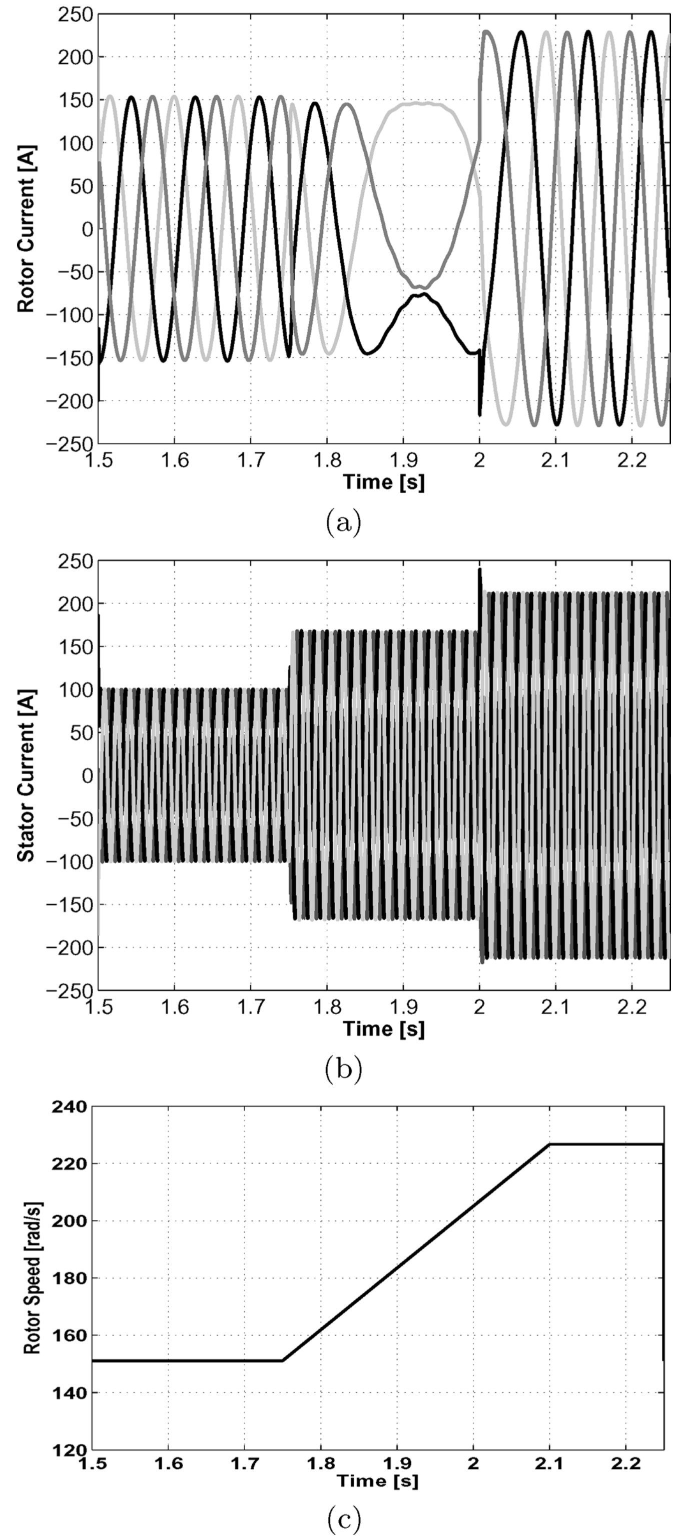


Fig. 10. Stator and rotor currents and rotor speed with several speed operation and parameters variations. (a) Rotor currents. (b) Stator currents. (c) Rotor speed.

resistance errors, the system maintains satisfactory performance and robustness under both steady-state and transient conditions.

## VI. Conclusion

This paper presented an MBPC applied to the DFIG power control. The control law is derived from optimization of an objective function that considers the control effort and the difference between the predicted outputs (active and reactive power) and the specific references. The predicted outputs were calculated using a linearized state-space model. This control law allows the calculation of the voltage to be applied on the rotor by using the system behavior for more than one single future sampling cycle. This strategy applies a constant switching frequency that overcomes the drawbacks of conventional DPC [18], [19].

The impact of machine parameter variations is analyzed and can be neglected. The simulations confirm the effectiveness and the robustness of the power controller during several operating conditions and variations of machine parameters. Thus, this power control strategy is an interesting tool for DFIG implementation.

## APPENDIX

*Effect of Parameters in the Rotor Voltage Calculation:* Considering that $L_{l1} \ll L_M$ and $L_{l2} \ll L_M$, the $\sigma L_2$ and $L_1/L_M$ can be simplified as

$$\begin{aligned}\sigma L_2 &= L_2 - \frac{L_M^2}{L_1} = \frac{L_1 L_2 - L_M^2}{L_1} = \\ &= \frac{(L_{l1}L_{l2}) + L_M(L_{l1}+L_{l2}) + L_M^2 - L_M^2}{L_{l1}+L_M} \cong \\ &\cong \frac{L_M(L_{l1}+L_{l2})}{L_M} = (L_{l1}+L_{l2})\end{aligned}$$

and

$$\frac{L_1}{L_M} = \frac{L_M + L_{l1}}{L_M} = 1 + \frac{L_{l1}}{L_M}.$$

*DFIG Parameters:* $R_1 = 0.02475\ \Omega$; $R_2 = 0.0133\ \Omega$; $L_m = 0.01425\ H$; $L_{l1} = 0.000284\ H$; $L_{l2} = 0.000284H\ H$; $J = 2.6\ \mathrm{Kg}\cdot\mathrm{m}^2$; $\mathrm{NP} = 2$; $PN = 149.2$ kVA; $V_N = 575$ V.

## REFERENCES


[1] M. G. Simões and F. A. Farret, *Renewable Energy Systems with Induction Generators*. Boca Raton, FL: CRC Press, 2004.

[2] R. Datta and V. T. Rangathan, "Variable-speed wind power generation using doubly fed wound rotor induction machine—A comparison with alternative schemes," *IEEE Trans. Energy Convers.*, vol. 17, no. 3, pp. 414–421, Sep. 2002.

[3] A. K. Jain and V. T. Ranganathan, "Wound rotor induction generator with sensorless control and integrated active filter for feeding nonlinear loads in a stand-alone grid," in *Proc. IEEE Power Electronics Specialists Conf. (PESC 2005)*, Jan. 2008, vol. 55, no. 1, pp. 218–228.

[4] B. H. Chowdhury and S. Chellapilla, "Double-fed induction generation control for variable speed wind power generation," *Electric Power Syst. Res.*, no. 76, pp. 786–800, 2006.

[5] B. Hopfensperger, D. J. Atkinson, and R. Lakin, "Stator-f lux-oriented control of a doubly-fed induction machine with and without position encoder," *Proc. Inst. Elect. Eng., Electr. Power Applications*, vol. 147, no. 4, pp. 241–250, Apr. 2000.

[6] B. Shen and B.-T. Ooi, "Novel sensorless decoupled p-q control of doubly-fed induction generator (DFIG) based on phase locking to $\gamma - \delta$ frame," in *Proc. IEEE Power Electronics Specialists Conf. (PESC 2005)*, Jun. 2005, pp. 2670–2675.

[7] A. Tapia, G. Tapia, J. X. Ostolaza, and J. R. Sáenz, "Modeling and control of a wind turbine driven doubly fed induction generator," *IEEE Trans. Energy Convers.*, vol. 18, no. 2, pp. 194–204, Jun. 2003.

[8] R. Peña, R. Cárdenas, J. Proboste, G. Asher, and J. Clare, "Sensorless control of doubly-fed induction generators using a rotor-current-based MRAS observer," *IEEE Trans. Ind. Electron.*, vol. 55, no. 1, pp. 330–339, Jan. 2008.

[9] J. P. da Costa, J. Marques, H. A. Gründling, and H. Pinheiro, "Dynamic behavior of the doubly-fed induction generator in stator flux vector reference frame," *Eletrônica de Potência*, vol. 13, no. 1, pp. 33–42, Mar. 2006.

[10] R. G. de Oliveira, J. L. da Silva, and S. R. Silva, "Development of a new reactive power control strategy in doubly-fed induction generators for wind turbines," *Eletrônica de Potência*, vol. 13, no. 4, pp. 277–284, Nov. 2008.

[11] F. Poitiers, T. Bouaouiche, and M. Machmoum, "Advanced control of a doubly-fed induction generator for wind energy conversion," *Electric Power Syst. Res.*, vol. 79, pp. 1085–1096, 2009.

[12] Z. Xin-fang, X. Da-ping, and L. Yi-bing, "Predictive functional control of a doubly fed induction generator for variable speed wind turbines," in *Proc. IEEE World Congress on Intelligent Control and Automation*, Jun. 2004, vol. 4, pp. 3315–3319.

[13] J. Morren, M. Sjoerd, and W. H. de Haan, "Ridethrough of wind turbines with doubly-fed induction generator during a voltage dip," *IEEE Trans. Energy Convers.*, vol. 20, no. 2, pp. 435–441, Jun. 2005.

[14] J. Guo, X. Cai, and Y. Gong, "Decoupled control of active and reactive power for a grid-connected doubly-fed induction generator," in *Proc. Third Int. Conf. Electric Utility Deregulation and Restructuring and Power Technologies (DRPT)*, Apr. 2008, pp. 2620–2625.

[15] X. Yao, Y. Jing, and Z. Xing, "Direct torque control of a doubly-fed wind generator based on grey-fuzzy logic," in *Proc. Int. Conf. Mechatronics and Automation (ICMA 2007)*, Aug. 2007, pp. 3587–3592.

[16] I. Takahashi and T. Noguchi, "A new quick-response and high-efficiency control strategy of an induction motor," *IEEE Trans. Ind. Appl.*, vol. IA-22, no. 5, pp. 820–827, Sep./Oct. 1986.

[17] M. Depenbrock, "Direct self-control (DSC) of inverter-fed induction machine," *IEEE Trans. Power Electron.*, vol. 3, no. 4, pp. 420–429, Oct. 1988.

[18] R. Datta and V. T. Ranganathan, "Direct power control of grid-connected wound rotor induction machine without rotor position sensors," *IEEE Trans. Power Electron.*, vol. 16, no. 3, pp. 390–399, May 2001.

[19] L. Xu and P. Cartwright, "Direct active and reactive power control of DFIG for wind energy generation," *IEEE Trans. Energy Convers.*, vol. 21, no. 3, pp. 750–758, Sep. 2006.

[20] D. Zhi and L. Xu, "Direct power control of DFIG with constant switching frequency and improved transient performance," *IEEE Trans. Energy Convers.*, vol. 22, no. 1, pp. 110–118, Mar. 2007.

[21] I. de Alegria, J. Andreu, P. Ibanez, J. L. Villate, and I. Gabiola, "Novel power error vector control for wind turbine with doubly fed induction generator," in *Proc. 30th Annu. Conf. IEEE Industrial Electronics Society, 2004 (IECON 2004)*, Nov. 2004, vol. 2, pp. 1218–1223.

[22] G. Xiao-Ming, S. Dan, H. Ben-Teng, and H. Ling-Ling, "Direct power control for wind-turbine driven doubly-fed induction generator with constant switch frequency," in *Proc. Int. Conf. Electrical Machines and Systems*, Oct. 2007, pp. 253–258.

[23] R. Kennel, A. Linder, and M. Linke, "Generalized predictive control (gpc)-ready for use in drive applications?," in *Proc. IEEE Power Electronics Specialists Conf. (PESC)*, 2001, vol. 4, pp. 1839–1844.

[24] H. Abu-Rub, J. Guzinski, Z. Krzeminski, and H. A. Toliyat, "Predictive current control of voltage-source inverters," *IEEE Trans. Ind. Electron.*, vol. 51, no. 3, pp. 585–593, Jun. 2004.

[25] L. Zhang, R. Norman, and W. Shepherd, "Long-range predictive control of current regulated PWM for induction motor drives using the synchronous reference frame," *IEEE Trans. Control Syst. Technol.*, vol. 5, no. 1, pp. 119–126, Jan. 1996.

[26] R. Kennel and A. Linder, "Direct model predictive control—A new direct predictive control strategy for electrical drives," in *Proc. Eur. Conf. Power Electronics and Applications*, 2005, 10 pp.

[27] A. Linder and R. Kennel, "Model predictive control for electrical drives," in *Proc. 36th IEEE Power Electronics Specialists Conf.*, Jun. 2005, pp. 1793–1799.

[28] E. S. de Santana, E. Bim, and W. C. do Amaral, "A predictive algorithm for controlling speed and rotor flux of induction motor," *IEEE Trans. Ind. Electron.*, vol. 55, no. 12, pp. 4398–4407, Dec. 2008.

[29] G. Abad, M. Ángel Rodríguez, and J. Poza, "Three-level npc converter-based predictive direct power control of the doubly fed induction machine at low constant switching frequency," *IEEE Trans. Ind. Electron.*, vol. 55, no. 12, pp. 4417–4429, Dec. 2008.

[30] W. Leonhard, *Control of Electrical Drives*. Berlin, Germany: Springer-Verlag, 1985.

[31] J. Holtz, J. Quan, J. Pontt, J. Rodríguez, P. newman, and H. Miranda, "Design of fast and robust current regulators for high-power drives based on complex state variables," *IEEE Trans. Ind. Appl.*, vol. 40, no. 5, pp. 1388–1397, Sep./Oct. 2004.

[32] A. J. S. Filho and E. Ruppert, "A deadbeat active and reactive power control for doubly-fed induction generator," *Electric Power Compon. Syst.*, vol. 38, no. 5, pp. 592–602, 2010.

[33] A. J. S. Filho and E. R. Filho, "The complex controller for three-phase induction motor direct torque control," *Sba Controle e Automação.*, vol. 20, no. 2, pp. 256–262, 2009.
[34] G. F. Franklin, J. D. Powel, and M. l. Workman, *Digital Control of Dynamic Systems*. Reading, MA: Addison-Wesley, 1994.
[35] J. A. Rossiter, *Model Based Predictive Control—A Practical Approach*. Boca Raton, FL: CRC Press, 2003.
[36] A. An, X. Hao, C. Zhao, and H. Su, "A pragmatic approach for selecting weight matrix coefficients in model predictive control algorithm and its application," in *Proc. IEEE Int. Conf. Automation and Logistics*, Aug. 2009, pp. 486–492.
[37] J. R. Rodríguez, J. W. Dixon, J. R. Espinoza, J. Pontt, and P. Lezana, "PWM regenerative rectifiers: State of the art," *IEEE Trans. Ind. Electron.*, vol. 52, no. 1, pp. 5–22, Feb. 2005.
[38] F. Blaabjerg, R. Teodorescu, M. Liserre, and A. V. Timbus, "Overview of control and grid synchronization for distributed power generation systems," *IEEE Trans. Ind. Electron.*, vol. 53, no. 5, pp. 1398–1409, Oct. 2006.

**Alfeu J. Sguarezi Filho** received the Bachelor's degree in electrical engineering from Faculdade Área 1 and the Master's degree from Campinas University, Brazil, in 2005 and 2007, respectively. He is currently working toward the Ph.D. degree at Campinas University.

His research interests are electrical machine drives, electrical power systems, power control, and doubly fed induction generator for disperse generation use.

**Milton E. de Oliveira Filho** was born in Bom Jesus da Lapa, Bahia, in 1966. He graduated as an electrical engineer from Universidade Federal de Itajubá, Itajubá, in 1995, and received the M.Sc. degree from the same university in 1998. He is working toward the Ph.D. degree at Campinas University, Brazil.

He is currently a designer engineer at General Electric Hydro Inepar, Campinas. His research interests are matrix converters, active power filters, and large power drives.

Mr. de Oliveira Filho has been a member of SOBRAEP since June 2007.

**Ernesto Ruppert Filho** received the Bachelor's degree in electrical engineering and the Master's and Ph.D. degrees from Campinas University, Brazil, in 1971, 1974, and 1983, respectively.

From 1972 to 1978, he was with the Electrical and Computer Enginneering School, Campinas University, as an Assistance Professor in the Electromechanical Energy Conversion area. From 1979 to 1983, he worked for General Electric in Brazil designing large induction and synchronous motors and working as an Application Engineer dedicated to large motors and generators. From 1983 to 1989, he worked for Vigesa Heavy Equipments in Brazil designig very large hydrogenerators and also performing commissionig testes in some hydro power plants in Brazil. From 1989 to 1992, he ran his own company dealing with electrical installations, and since 1992 he has been working as a Full Professor at the Electrical and Computer Engineering School, Campinas University, Campinas, Brazil, researching and teaching in the areas of electrical machines, power electronics, drives, and electrical power systems.